Collective excitations in metal-ammonia systems as a function of electron density

A. H. Said,[1,2] C. A. Burns,[2] E. E. Alp,[1] H. Sinn,[1] and A. Alatas[1]
[1]*Argonne National Laboratory, Argonne, Illinois 60439, USA*
[2]*Western Michigan University, Kalmazoo, Michigan 49008, USA*
(Received 22 April 2003; published 18 September 2003)

We report measurements of the ionic collective excitations of a metal-ammonia system [lithium-ammonia with 20, 16, 13 mole % metal (MPM) at $T=240$ K and sodium-ammonia with 18, 14, 10 MPM at $T=222$ K]. These data were analyzed to determine the acoustic collective excitation dispersion relation and the linewidth. Deviations from the Bohm-Staver model for electron-ion coupling are discussed for the low electronic densities found in these systems.

DOI: 10.1103/PhysRevB.68.104302 PACS number(s): 61.25.Mv, 63.20.Kr, 78.70.Ck

I. INTRODUCTION

Alkali metals dissolve in liquid ammonia without chemical reaction, resulting in a free electron and a positively charged alkali-metal ion. Solutions of alkali metals in liquid ammonia have been the subject of many experimental and theoretical investigations,[1,2] for over a century.

The properties of metal-ammonia solutions depend on the concentration of the metal. For instance, the solution undergoes a metal-insulator transition with 3–8 mole % metal[2] (MPM) and is metallic for concentrations above 8 MPM.[3] The solution saturates at ~20 MPM for lithium-ammonia and 17.5 MPM for the sodium-ammonia solutions.[4] At saturation, the Li-NH_3 solution has an electrical conductivity about three times that of Na-NH_3 and about 1% that of copper. Metal-ammonia solutions have a measured macroscopic viscosity about ten times lower than that of typical liquid metals.[5]

Neutron-diffraction[6–8] studies of saturated liquid lithium-ammonia and saturated solid lithium-ammonia,[9] as well as nuclear-magnetic-resonance measurements of self-diffusion,[10] show that the lithium ion is coordinated by four ammonia molecules and this coordination number is independent of concentration.[11] For the sodium-ammonia solution, a recent study of the structure of the saturated solution showed that the sodium ions are solvated by 4.7 (~5) ammonia molecules.[4]

Recently, studies[12,13] of the plasmon in liquid lithium-ammonia as a function of concentration and in solid lithium-ammonia have been used to look for the breakdown of the random-phase approximation (RPA) at low electron densities. Strong deviations from the RPA were found, with greatest deviations at the lowest electronic densities. The dispersion for the acoustic collective excitations has been measured[14] using inelastic x-ray scattering (IXS) for a saturated lithium-ammonia solution. The measurement showed a softening in the dispersion at twice the Fermi wave vector $2k_F$, and the system was speculated to be close to a transition related to electronic ordering. Neutron scattering has also been carried out on the saturated lithium-ammonia solution[15] to measure the collective excitation dispersion, and a similar trend was observed.

The electron density in metals helps to determine the importance of the electronic interactions, which can play a critical role in their properties. Usually electron density is described by the dimensionless parameter

$$r_s=\frac{1}{(4\pi n/3)^{1/3}a_0}, \tag{1}$$

where n is the free electron density and a_0 is the Bohr radius. Since the Fermi (kinetic) energy for the electron gas falls off as $1/r_s^2$, while the Coulomb energy goes as $1/r_s$, the lower the electronic density, the greater the importance of electron-electron interactions compared to kinetic energy.

Metallic lithium-ammonia and sodium-ammonia systems have values of $r_s \approx 7.4$–12, substantially larger than that of the common metals, which have values of 2–6. By changing the metal concentrations, we can easily reach any desired value of r_s, which makes this system valuable for testing theoretical calculations at low electron density.

Collective excitations in liquid alkali metals [Rb,[16] Cs,[17] Na,[18,19] and Li (Refs. 20,21)] and other liquids [H_2 (Ref. 22) and NH_3 (Ref. 23)] have been studied using neutron and x-ray scattering. The studies showed well-defined excitations beyond the hydrodynamic regime ($\lambda \gg 2\pi/Q_0$). The modes disperse linearly at low Q and reach a maximum around $Q_0/2$ (Q_0 is the position of the first maximum in the static structure factor). In liquid metals,[16–21] the modes showed dips near Q_0.

We have studied the collective excitations in liquid lithium-ammonia and sodium-ammonia using IXS for different concentrations of 10–20 MPM, which correspond to r_s between 9.2 and 7.4.

II. EXPERIMENT

The experiments were carried out at the high-resolution inelastic x-ray scattering beam line 3ID-C at the Advanced Photon Source (APS). Experiments were done at two different energy resolutions. For the saturated sodium-ammonia solution, the synchrotron beam was monochromatized by a diamond double-crystal monochromator at energy of 25.701 keV. This beam was further monochromatized by two silicon nested channel cuts[24] and focused by a total-reflecting mirror to a spot size at the sample of 300 μm horizontally and 250 μm vertically. A temperature controlled (to within 20

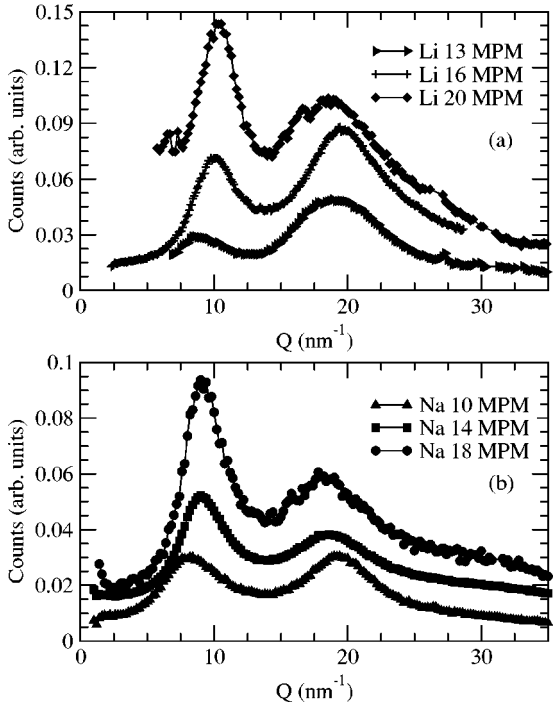

FIG. 1. Static structure factor for (a) Li-ammonia and (b) Na-ammonia at different concentrations. Data have been offset for clarity.

mK), spherically bent and diced Si (13 13 13) analyzer was used to reflect the scattered x rays onto a cadmium zinc telluride semiconductoring detector 6 m away from the analyzer and 3 mm offset from the incident beam. The total experimental energy resolution was measured using the elastic scattering from a Plexiglas sample and found to be 1.4 meV. The setup for the experiment is described in more detail in Refs. 25 and 26

For the lithium-ammonia solutions (13, 16, 20 MPM) and two of the sodium-ammonia solutions (10, 14 MPM), we used the same setup with an incident energy of 21.657 keV and a Si (18 6 0) analyzer. The total energy resolution was measured to be 2 meV.[25] The 2 meV setup has a higher flux (30 times more). Energy scans were made by rotating the inner and outer crystals of the nested monochromator.

The sample containers were stainless-steel cells with two thin (35 μm), flat beryllium windows. In a helium-filled glove box, 99.95% pure sodium and 99.9% pure lithium were cut, weighed, and then placed into the sample cells. For the lithium solutions, a measured volume of high purity 99.99% anhydrous ammonia was condensed in the cell at $T \sim 200$ K. The cell was sealed off and placed in a helium flow cryostat and kept at $T \approx 240$ K. For the sodium-ammonia solutions, we used a different cell that was designed to condense the 99.99% anhydrous ammonia after cooling the cell inside the cryostat. The sample path length was 12 mm for the lithium mixtures and 10 mm for the sodium solutions. The sodium-ammonia solutions were kept at $T \approx 222$ K.

The static structure factor $S(Q)$, as shown in Fig. 1, was measured for all concentrations before, during, and after measuring the IXS spectra to confirm the stability of the solutions during the measurements. No change was seen in the $S(Q)$, indicating the samples were stable during the measurements. The IXS measurements for the empty cell reveal a negligible contribution to our data. However, the beryllium windows show small powder-diffraction peaks in $S(Q)$ around 32 nm^{-1}, which were removed from the $S(Q)$ data.

We measured $S(Q,\omega)$ in the Q range between 1.5 nm^{-1} and 16 nm^{-1} and an energy range of ± 40 meV, finding a well-defined acoustic mode at low energy transfer (<10 meV). The IXS data for all concentrations at different Q values are shown in Figs. 2–8; the points are our data, the solid lines are the fitting curve, and the dotted lines are the measured resolution functions of the instrument.

The raw $S(Q)$ data are shown in Fig. 1, normalized to the intensity of the incident beam. No other corrections were made. The $S(Q)$ measurements show two peaks around 9 nm^{-1} and $Q = 18$ nm^{-1} for the Na-NH_3, and 10 nm^{-1}

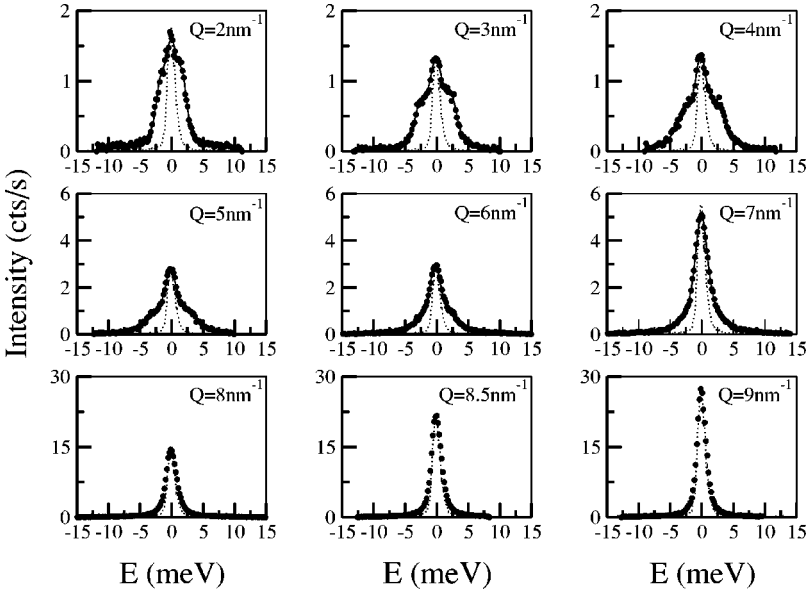

FIG. 2. The IXS data for Na 18 MPM.

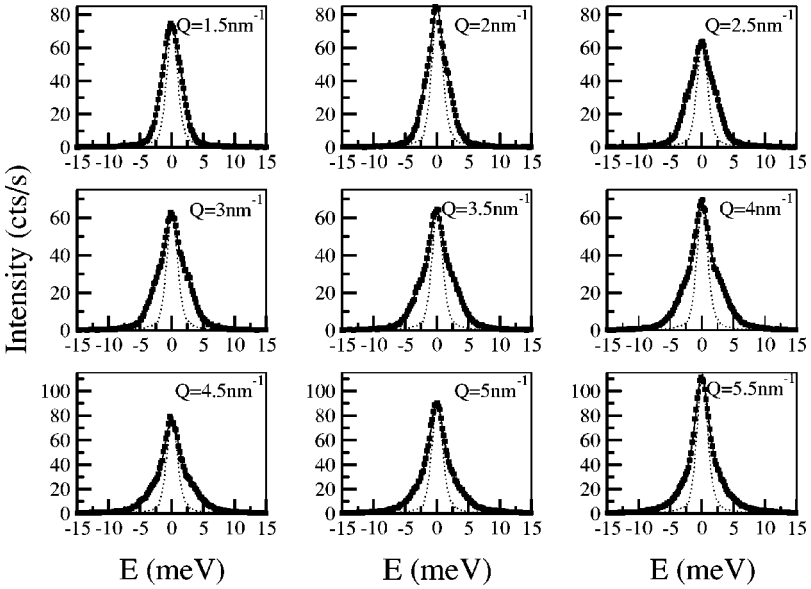

FIG. 3. The IXS data for Na 14 MPM at low Q.

and 18 nm^{-1} for Li-NH_3. Neutron-scattering studies[4,6,7] showed $S(Q)$ behavior similar to ours. The appearance of the first peak in $S(Q)$ in both the lithium-ammonia and sodium-ammonia solutions is an indication of intermediate range ordering. The first peak is related to correlation between the metal-ammonia complexes and is absent in $S(Q)$ measurements for pure ammonia. The position of the first peak for both saturated solutions is very close to $2k_F$ of the system, but, at low concentration, the position of the peak is slightly larger than twice the Fermi wave vector. The second peak is related to the N-N correlation. The measured $S(Q)$ show a shift to lower Q and a drop in the intensity of the first peak as we lower the metal concentration. The second peak shifts to lower Q upon increasing the metal concentration. The shift occurs as a result of the increase in the distance between the ammonia molecules due to the presence of solvated ions and electrons[7] as the concentration is increased.

The IXS data shown in Figs. 2–8 have well-defined peaks at the highest electron density for both saturated solutions; these peaks are clearly seen at low Q up to $Q \approx Q_0/2$. At lower electron density (the other concentrations), the modes are not well-defined side peaks but are merged with the central peak resulting in a broadening compared to the resolution function. At Q close to Q_0, the peaks narrow, and they are not distinguishable from the resolution function; however, the peaks become broad again for $Q > Q_0$.

We found the modes are better defined for saturated lithium-ammonia than for saturated sodium-ammonia. Other modes also appear at higher energies (around 9, 18, 27, 40 meV) as a result of vibration modes for the alkali ion ammonia complexes. While these peaks become more pronounced at higher Q, they are never very intense. These modes will be discussed in more detail elsewhere.[27] The modes for saturated lithium-ammonia solution are shown in Fig. 9.

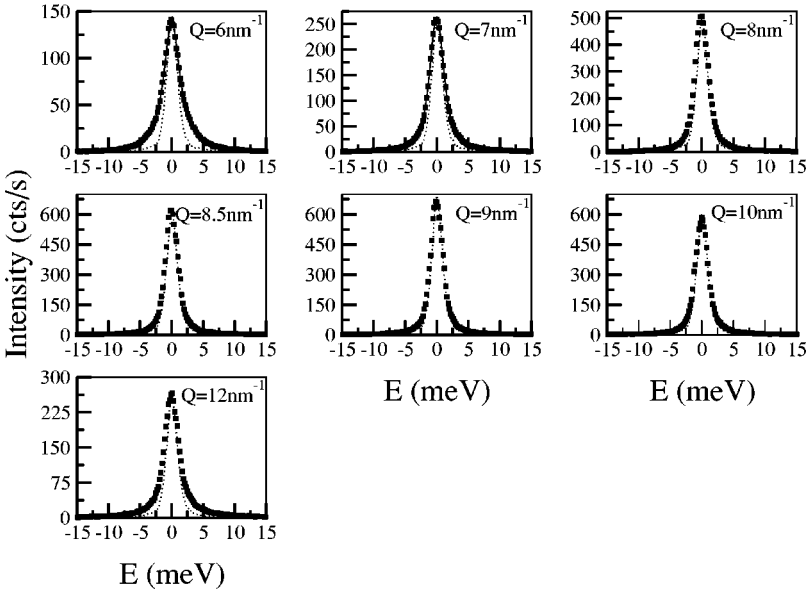

FIG. 4. The IXS data for Na 14 MPM at high Q.

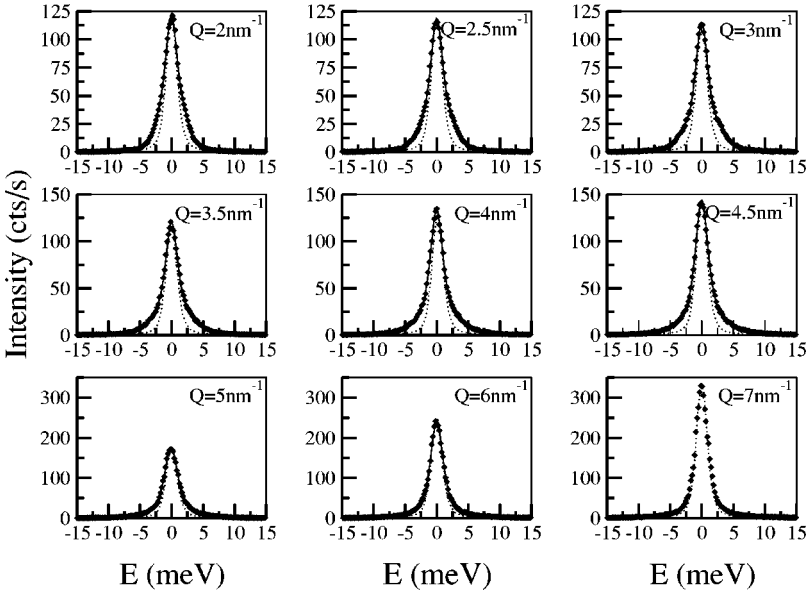

FIG. 5. The IXS data for Na 10 MPM.

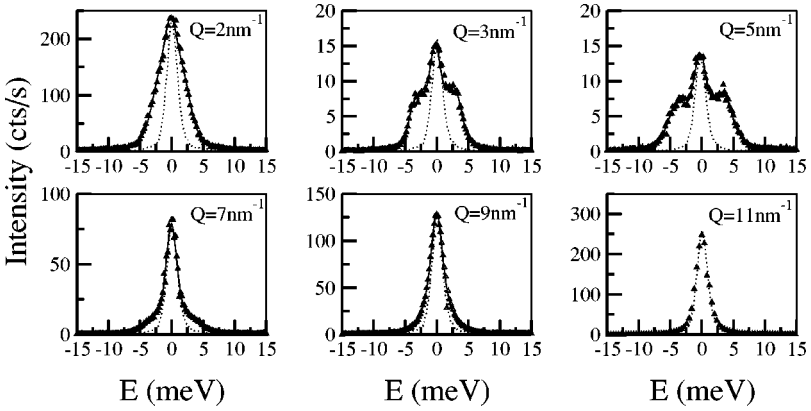

FIG. 6. The IXS data for Li 20 MPM.

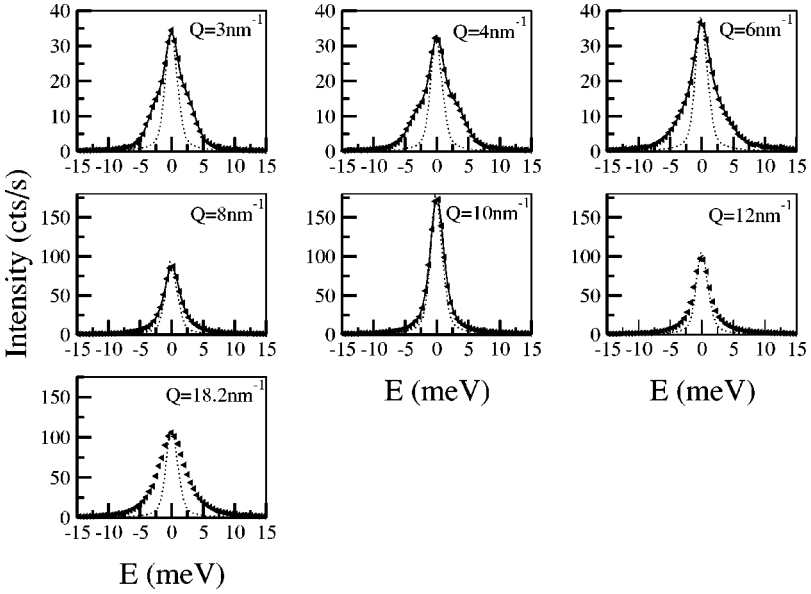

FIG. 7. The IXS data for Li 16 MPM.

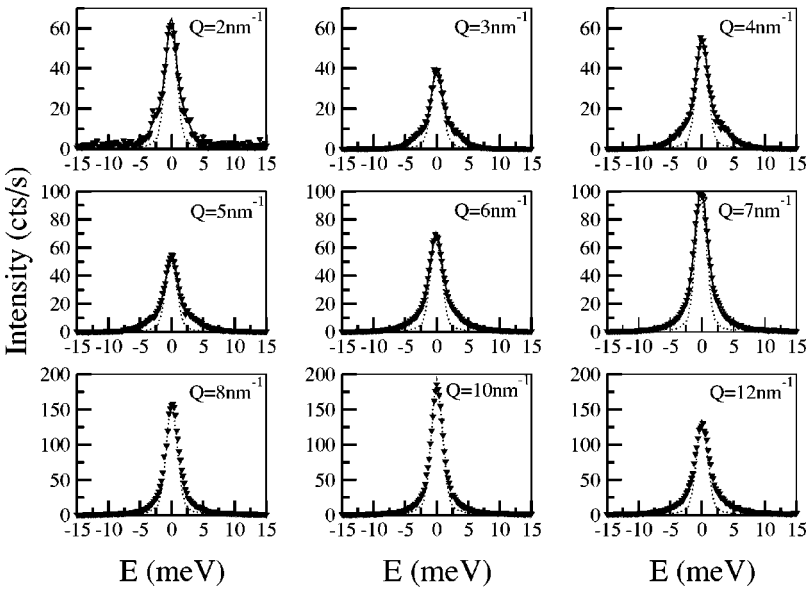

FIG. 8. The IXS data for Li 13 MPM

III. DATA ANALYSIS

We have used the damped harmonic oscillation function convoluted with the instrumental resolution function to fit the acoustic modes in our data. The fitting function $F(Q,\omega)$ is defined as

$$F(Q,\omega)=I_0(Q)\frac{\Gamma_0(Q)}{\Gamma_0^2(Q)+\omega^2}+[n(\omega)+1]I(Q)$$

$$\times\frac{4\omega\Gamma(Q)\Omega(Q)}{[\Omega^2(Q)-\omega^2]^2+4\Gamma^2(Q)\omega^2}+\sum_i L_i. \quad (2)$$

The first term is a Lorentzian function to fit the central peak, and the second term fits the two side peaks that are the acoustic modes. Here I is the intensity of the side peaks, Γ is the half width at half maximum of the peak, Ω is the energy of the side peaks, and $n(\omega)$ is the thermal occupation factor. The subscripts 0 correspond to the same variables but for the central peak. The last term represents a sum of Lorentzian functions (usually two of them), which we added to our fitting function to fit the optical modes (see Fig. 9), which have a very low intensity compared to the acoustic modes. They affect our fitting by altering the tail of the side peak, which reduces the ability to fit the tails. By adding these Lorentzians the fit becomes more stable, but the results are not fundamentally different than without them.

We have also used other models to fit the data, such as the extended hydrodynamic model[28] and the generalized three effective eigen-mode model;[29] all of them gave equivalent results.

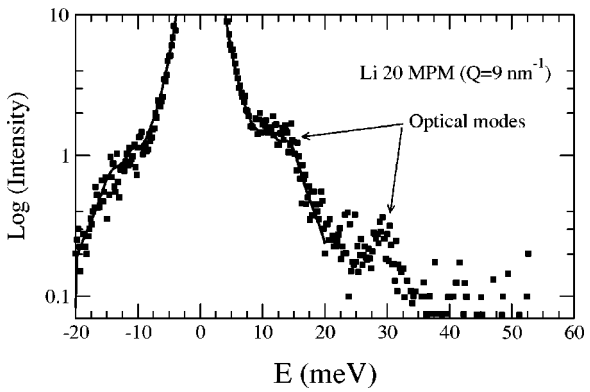

FIG. 9. The IXS data for Li 20 MPM at $Q=9$ nm^{-1}, showing the optical modes. The dots are our data and the solid line is the fit (described below).

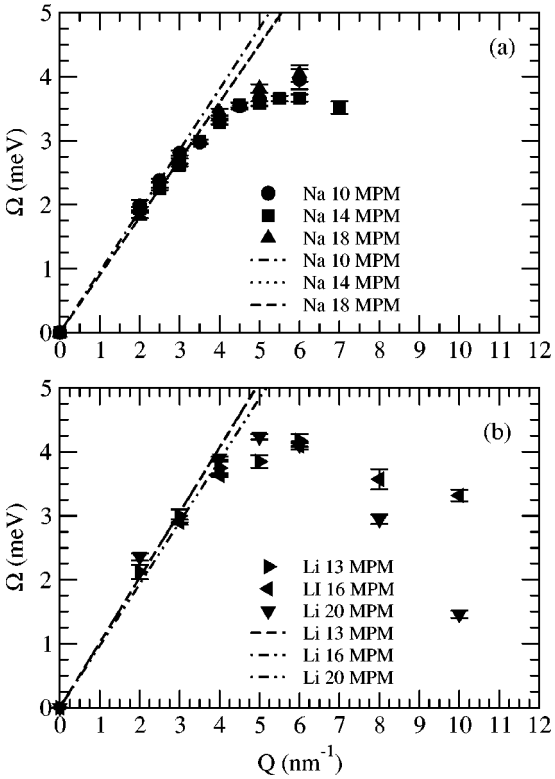

FIG. 10. The dispersion relation for (a) Na-ammonia and (b) Li-ammonia. The dashed lines are linear fits to the low Q dispersions.

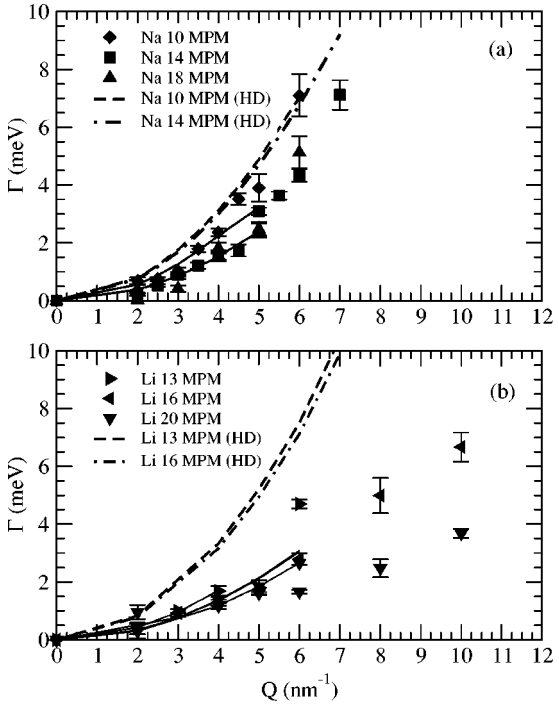

FIG. 11. The linewidths for (a) Na-ammonia and (b) Li-ammonia. The solid lines are the quadratic fits to the low Q linewidths. The dashed lines are the hydrodynamics calculations.

The fitting parameters $\Omega(Q)$ and Γ are shown in Figs. 10 and 11, respectively. At low Q, a linear dispersion in $\Omega(Q)$ is observed for all concentrations, which is expected for a soundlike mode. The fitting results for the linear Q dependence for the acoustic modes are shown in Fig. 10 as thin dashed lines. The slopes of the linear dispersion are comparable to the adiabatic sound velocity measured by ultrasound[6] as shown in Table I.

The dispersion relations for sodium-ammonia, Fig. 10(a), show similar behavior for the measured concentrations, with the modes dispersing linearly at low Q and reaching a maximum around $Q_0/2$. The Q dependence of the linewidth [Fig. 11(a)], which is proportional to the inverse of the lifetime of the collective excitations, indicates a shorter lifetime as the metal concentration is decreased. However, the modes become overdamped at higher Q as we approach Q_0. Increased disorder in the system upon lowering the metal concentration may be the reason for the strong damping at the lower concentrations. For lithium-ammonia solutions, the dispersion relations in Fig. 10(b) show linear dispersion at low Q and maximum energy around $Q_0/2$. The lifetime is proportional to the metal concentration in the system as shown in Fig. 11(b).

Comparing sodium-ammonia and lithium-ammonia, we see similar behavior for the linewidth. The collective excitations in sodium-ammonia solution have a slightly lower energy than those in lithium-ammonia due to the difference in the masses. Also the modes propagate to higher Q in the lithium-ammonia compared to the sodium-ammonia. The Q-dependence linewidth shows a shorter lifetime for the sodium-ammonia solution than for the lithium-ammonia. In the concentration range we measured, we do not see any sudden change of the behavior of the dispersion relation. However, we might expect a change at lower concentration, where the system is not a good metal. Such a change would be more visible when we pass through the metal-insulator transition, where the conduction electrons become localized. Sound velocity measurements indeed show a rapid change at a concentration lower than 8 MPM.[5]

The hydrodynamic model predicts a quadratic Q dependence for the damping, which is related to the longitudinal kinematic viscosity of the system as[30]

$$\Gamma(Q)=\frac{1}{2}\nu_l Q^2, \tag{3}$$

where $\nu_l=\eta_l/\rho$ is the longitudinal kinematic viscosity, $\eta_l=4\eta/3+\eta_B$ is the longitudinal viscosity, η is the shear viscosity, η_B is the bulk viscosity, and ρ is the mass density. The macroscopic measurements[5] show a decrease in the viscosity as the metal concentration increases.

We compared the damping parameter calculated from the hydrodynamic and our data. The bulk viscosity can have any value from much smaller than the shear viscosity to several times the shear viscosity. As an approximation, we have used $\eta_B=\eta$ (no data exist for the bulk viscosity).

TABLE I. Sound velocities for different metal-ammonia concentrations. The adiabatic sound velocities are taken from Ref. 5, and the Bohm-Staver sound velocities are calculated from Eq. (6). The dimensionless parameter α is calculated from the ratio between experimental and theoretical [Arnold and Paterson calculations (Ref. 34)] values of electrical conductivity, leading to the sound velocity calculated from Eq. (8). The damping constants are calculated from hydrodynamics and from the linewidth of the collective excitations in our data.

Metal-ammonia (MPM)	Adiabatic sound velocity (m/s)	Sound velocity from our data (m/s)	Sound velocity calculated from BS model (m/s)	α	Sound velocity from Eq. (8) (m/s)	$\Gamma(Q)$ calculated from hydrodynamics (meV)	$\Gamma(Q)$ fitted from our data (meV)
Li 13	1450 ± 25	1550 ± 70	780	0.29	1380	$(0.208\pm0.003)Q^2$	$(0.10\pm0.02)Q^2$
Li 16	1450 ± 20	1470 ± 80	830	0.22	1280	$(0.198\pm0.003)Q^2$	$(0.09\pm0.02)Q^2$
Li 20	1460 ± 15	1540 ± 100	890	0.13	1060	No data	$(0.07\pm0.02)Q^2$
Na 10	1400 ± 20	1450 ± 60	590	0.52	920	$(0.195\pm0.003)Q^2$	$(0.14\pm0.02)Q^2$
Na 14	1340 ± 20	1410 ± 70	660	0.3	780	$(0.188\pm0.003)Q^2$	$(0.10\pm0.02)Q^2$
Na 18	1340 ± 20	1370 ± 40	700	0.28	800	No data	$(0.10\pm0.02)Q^2$

The calculated values for Γ are shown in Table I and in Fig. 11 with the dashed lines. For the 13 MPM lithium-ammonia solution, the damping constant calculated from hydrodynamics is about a factor of 2 higher than the fit from our data. Furthermore, the difference between both values (hydrodynamic and our data) increases for the 16 MPM lithium-ammonia solution. For the 10 MPM sodium-ammonia solution, we see better agreement between the damping constant calculated from hydrodynamics and our fitted value; however, the hydrodynamics result is about two times higher than our fitted values for the 14 MPM sodium-ammonia solution. The discrepancy between the macroscopic observed viscosity and the damping constants observed in our experiment is likely due to a viscoelastic relaxation[31] leading to reduced viscosity at high frequencies. However, compared to other liquid metals, we see better agreement between the measured damping constant for our data and that calculated from the hydrodynamic calculation.[17]

As a first approximation for the dispersion, we compare our results to the Bohm-Staver (BS) model,[32] which considers the metals as a gas of pointlike ions interacting through the Coulomb potential screened by the electron gas. As a result of the screening, the long-wavelength frequency of longitudinal collective excitations Ω_P, ion plasma frequency, is reduced by $1/\sqrt{\epsilon(Q)}$,

$$\omega^2(Q)=\frac{\Omega_P^2}{\epsilon(Q)}, \tag{4}$$

where $\Omega_P^2=4\pi n_i(Ze)^2/M$, n_i is the ion number density, Z is the number of valence electrons, M is the ion mass, e is the electron charge, and $\epsilon(Q)$ is the electron-gas dielectric constant. As $Q\rightarrow 0$,[33]

$$\lim_{Q\rightarrow 0}\epsilon(Q)=1+\frac{q_{TF}^2}{Q^2}\frac{K}{K_f}, \tag{5}$$

where $q_{TF}^2=6\pi e^2 n_e/E_F$ is the Thomas-Fermi screening wave vector, E_F is the Fermi energy, K is the compressibility of the system, and $K_f=3/(2nE_F)$ is the free-electron compressibility. In the RPA, $K/K_f=1$, so the sound velocity is given by

$$v_s=\lim_{Q\rightarrow 0}\sqrt{\frac{\Omega_P^2}{Q^2\epsilon(Q)}}=\sqrt{\frac{m_0 Z}{3M}}v_F, \tag{6}$$

where m_0 is the mass of a free electron and v_F is the velocity of the electron at the Fermi surface. This relationship is commonly used to explain the presence of an acoustic sound mode with linear dispersion in metals.

We have applied this model to our system as shown in Table I, and we have found that the calculations of sound velocity neither agree with the measured sound velocity[5] nor with the ion-acoustic velocity. As an ion mass M, we took the mass of the complex (one lithium and four ammonia molecules and one sodium and five ammonia molecules). Another way of treating the system is by considering the interaction between the bare ions. The effect of the ammonia molecules can be taken into account by introducing their dielectric constant. This was done by Arnold and Patterson[34] to calculate the conductivity of metal-ammonia mixtures. Lagowski and Sienko[5] attempted to reconcile the calculated electric conductivity and the experimental values by introducing a varying ratio between the effective mass of the electron m and the dielectric constant of the medium ϵ as

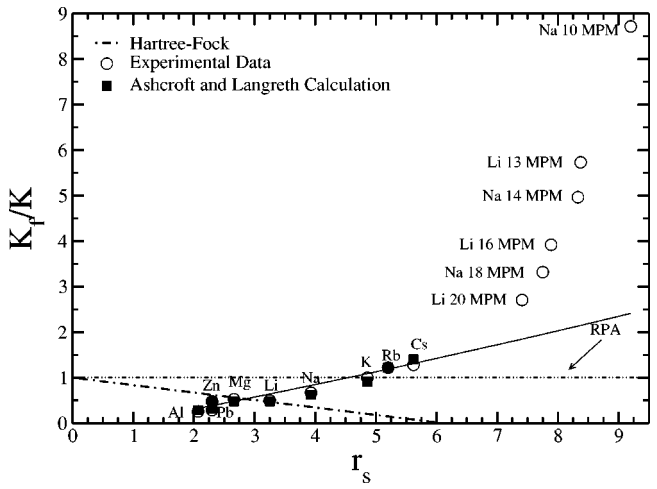

FIG. 12. Comparison of experimental and theoretical values of the compressibility K. The open circles are the experimental values. The solid squares are the values calculated by Ashcroft and Langreth (Ref. 35) The solid line is the Ashcroft and Langreth calculation ignoring the band-structure effects.

$$(m/\epsilon)=\alpha(m_0/\epsilon_0), \tag{7}$$

where α is a dimensionless parameter that varies with the concentration and ϵ_0 is the optical dielectric constant of NH_3. By considering the effect of the effective mass of the electron and the dielectric constant of the medium in BS model, we end up with

$$v_s^{bare}=\alpha^{1/2}\sqrt{\frac{m_0 Z}{3M_{bare}}}v_F, \tag{8}$$

where M_{bare} is the mass of the bare ion.

We calculated the sound velocity from Eq. (8) as shown in Table I. The calculations show an improved agreement and a similar trend with changing metal concentrations. However, the calculated sound velocities remain still significantly below the experimental value. The failure of the BS model to explain the electron-ion coupling at low electron density is due to several factors. The electron-electron interaction becomes more significant at low electron density, where the kinetic energy of the electrons become smaller compared to systems with high electron density. The RPA considers $K/K_f=1$, therefore the noninteracting electrons are responsible for the compressibility of the system, but the theoretical calculations[35] and the experimental data[33] show deviations from RPA at low and high electron densities, as shown in Fig. 12. Our study seems to indicate that the dielectric constant is a slowly varying function of r_s and perhaps has a lower value than the one calculated by RPA. Ashcroft and Langreth[35] have calculated the interacting electron-gas com-

pressibility based on perturbation theory. The exchange energy, correlation energy, electron-ion interaction, ion-ion interaction, and band-structure effects were considered in their calculations. They have found a good agreement with the experimental values for simple metals. Using their calculation and ignoring the band-structure effect, we have calculated K_f/K at low electron density as shown with the solid line in Fig. 12. Our data show a qualitative trend similar to the calculated values.

IV. CONCLUSION

In conclusion, we have carried out high-resolution inelastic x-ray-scattering measurements on lithium-ammonia and sodium-ammonia systems as a function of concentration. We see well-defined phononlike excitations to large momentum transfers. Their linewidth increases at large momentum transfer. We compared the damping constant calculated from the hydrodynamic model and the fitted value to our data, and we found good agreement between the hydrodynamic model and the sodium-ammonia solution at 10 MPM. However, the hydrodynamic damping constant is about two times higher than the experimental value for the 14 MPM sodium solution and (13, 16) MPM lithium-ammonia. This study shows the acoustic dispersion relations and the lifetime behavior for these systems. At low electron densities, we see evidence that the value of dielectric constant is smaller than the value calculated within the RPA.

ACKNOWLEDGMENTS

We would like to thank Dr. Arthur J. Kahaian, Transportation Technology R&D Center, Argonne National Laboratory, for helping us to use the glove box in his laboratory. This work was supported by the U.S. Department of Energy (DOE), Division of Material Science, Grant No. DE-FG02-99ER45772, and sector 3 at the APS, which was supported by the DOE, Office of Energy Research, under Contract No. W-31-109-ENG-38.

[1] J. Jortner and N. Kestner, *Electrons in Fluids* (Springer-Verlag, New York, 1973).
[2] J. Thompson, *Electrons in Liquid Ammonia* (Clarendon, Oxford, 1976).
[3] R. Schroeder and J. Thompson, Phys. Rev. **179**, 124 (1969).
[4] J.C. Wasse, S.L. Stebbings, S. Masmanidis, S. Hayama, and N.T. Skipper, J. Molecular Liquids **96-97**, 341 (2002).
[5] J. J. Lagowski and M. J. Sienko, *Metal-Ammonia Solutions* (Butterworths, London, 1970).
[6] J.C. Wasse, S. Hayama, and N.T. Skipper, Phys. Rev. B **61**, 11 993 (2000).
[7] J.C. Wasse, S. Hayama, and T. Skipper, J. Chem. Phys. **112**, 7147 (2000).
[8] J.C. Wasse, S. Hayama, S. Masmanidis, S.L. Stebbings, and N.T. Skipper, J. Chem. Phys. **118**, 7486 (2003).
[9] N. Mammano and M.J. Sienko, J. Am. Chem. Soc. **90**, 6322 (1968).
[10] A. Garroway and R.M. Cotts, Phys. Rev. A **7**, 635 (1973).
[11] S. Hayama, N.T. Skipper, J.C. Wasse, and H. Thompson, J. Chem. Phys. **116**, 2991 (2002).
[12] C. Burns, P. Giura, A. Said, A. Shukla, G. Vankó, M. Tuel-Benckendorf, E. Isaacs, and P. Platzman, Phys. Rev. Lett. **89**, 236404 (2002).
[13] H. Hayashi, Y. Udagawa, C.C. Kao, J.P. Rueff, and F. Sette, J. Electron Spectrosc. Relat. Phenom. **120**, 113 (2001).
[14] C. Burns, P. Platzman, H. Sinn, A. Alatas, and E. Alp, Phys. Rev. Lett. **86**, 2357 (2001).
[15] F. Sacchetti, E. Guarini, C. Petrillo, L.E. Bove, B. Dorner, F. Demmel, and F. Barocchi, Phys. Rev. B **67**, 014207 (2003).
[16] J. Copley and J. Rowe, Phys. Rev. Lett. **32**, 49 (1974).
[17] T. Bodensteiner, C. Morkel, W. Glöser, and B. Dorner, Phys. Rev. A **45**, 5709 (1992).
[18] T. Scopigno, U. Balucani, G. Ruocco, and F. Sette, Phys. Rev. E **65**, 031205 (2002).
[19] W.C. Pilgrim, S. Hosokawa, H. Saggau, H. Sinn, and E. Burkel, J. Non-Cryst. Solids **250-252**, 96 (1999).
[20] H. Sinn, F. Sette, U. Bergmann, C. Halcoussis, M. Krisch, R. Verbeni, and E. Burkel, Phys. Rev. Lett. **78**, 1715 (1997).
[21] T. Scopigno, U. Balucani, G. Ruocco, and F. Sette, Phys. Rev. Lett. **85**, 4076 (2000).
[22] F.J. Bermejo, K. Kinugawa, C. Cabrillo, S.M. Bennington, B. Fåk, M.T. Fernández-Díaz, P. Verkerk, J. Dawidowski, and R. Fernández-Perea, Phys. Rev. Lett. **84**, 5359 (2000).
[23] F. Sette, G. Ruocco, A. Cunsolo, C. Masciovecchio, G. Monaco, and R. Verbeni, Phys. Rev. Lett. **84**, 4136 (2000).
[24] T.S. Toellner, Hyperfine Interact. **125**, 3 (2000).
[25] H. Sinn *et al.*, Nucl. Instrum. Methods Phys. Res. A **467-468**, 1545 (2001).
[26] H. Sinn, J. Phys.: Condens. Matter **13**, 7525 (2001).
[27] C. A. Burns, G. Vankó, H. Sinn, A. Alatas, E. E. Alp, and A. H. Said (unpublished).
[28] I. de Schepper, P. Verkerk, A.A.V. Well, and L. de Graaf, Phys. Rev. Lett. **50**, 974 (1983).
[29] P. Chen, S. H. Chen, T. Weiss, H. Huang, H. Sinn, and E. Alp (unpublished).
[30] J. Boon and S. Yip, *Molecular Hydrodynamics* (Dover, New York, 1980).
[31] S.E. Lovesey, J. Phys. C **4**, 3057 (1971).
[32] N. March and M. Tosi, *Coulomb Liquids* (Academic Press, London, 1984).
[33] G. D. Mahan, *Many-Particle Physics* (Plenum, New York, 2000).
[34] E. Arnold and A. Patterson, J. Chem. Phys. **41**, 3089 (1964).
[35] N. Ashcroft and D.C. Langreth, Phys. Rev. **155**, 682 (1967).